Numerical Solution of Steady Free-Surface Navier-Stokes Flow

Harald van Brummelen*, Hoyte Raven†

Abstract

The usual time integration approach for solving steady viscous free surface flow problems has several drawbacks. We propose instead an efficient iterative method, which relies on a different but equivalent formulation of the free surface flow problem, involving a so-called quasi free-surface condition. Furthermore, we present a method for analyzing the properties of wave solutions of the discrete equations. Numerical results for flow over a bottom bump agree well with measurements and with the predictions of the analysis.

1 Introduction

The numerical solution of flows which are partially bounded by a freely moving boundary is of great practical importance. Current methods for solving steady viscous free-surface flow problems typically display two defects, viz., high computational costs due to persistent transient behavior and substantial numerical damping of gravity wave solutions. In the present work we address both of these problems.

To reduce the computational effort of solving the steady free-surface flow problem, we propose an efficient iterative solution method. Whereas dedicated techniques have been developed for the solution of steady free surface potential flow [2, 4], methods for steady Navier-Stokes flow simply continue the usual time integration process until a steady state is reached. In [5] several drawbacks of this process are discussed, such as slow convergence to steady state. In particular, one can show that at subcritical Froude numbers, dispersion causes asymptotic temporal behavior of the amplitude of transient waves in $\mathbb{R}^d$ of $O(t^{-(d-1)/2})$. Hence, if the objective is to reduce the amplitude of transient waves to the order of spatial discretization errors, the efficiency of the time integration approach deteriorates rapidly with decreasing meshwidth. In practical computations, thousands of time steps are usually required.

The iterative method we propose relies on a different but equivalent formulation of the free-surface flow problem, involving a quasi free-surface condition. The method solves a sequence of steady Navier-Stokes subproblems with this condition imposed at an approximation to the steady free boundary. Each subproblem evaluation yields an improved approximation to the steady free surface position. For the testcase presented, the method displays linear convergence of the boundary location and the results exhibit good agreement with measurements.

To reduce numerical wave damping, a priori knowledge of the properties of the discretization scheme is imperative. We present a method for analyzing the properties of the discretized equations corresponding to the subproblems. The analysis yields valuable information on numerical wave damping and dispersion and can serve in the assessment of discretization schemes. The results of the analysis agree well with the computed results.

2 Problem Statement & Solution Method

We consider an incompressible, viscous fluid flow, subject to a constant gravitational force on a domain, $\mathcal{V}$. The domain is bounded by a free boundary, $\mathcal{S}$, and fixed boundaries $\partial\mathcal{V} \setminus \mathcal{S}$. The flow is characterized by the Froude number, Fr, and the Reynolds number, Re. The (nondimensionalized) fluid velocity and pressure are identified by $\mathbf{v}(\mathbf{x})$ and $p(\mathbf{x})$, respectively. The objective is to find $\mathcal{V}, \mathbf{v}(\mathbf{x}), p(\mathbf{x})$ such that the steady (Reynolds Averaged) Navier-Stokes equations are satisfied on $\mathcal{V}$, the appropriate boundary conditions hold at fixed boundaries and, moreover, at the free surface the steady kinematic condition,

$$\mathbf{v}\cdot\mathbf{n} = 0, \qquad \mathbf{x} \in \mathcal{S}, \tag{1}$$

*CWI, P.O. Box 94079, 1090 GB Amsterdam, The Netherlands
†MARIN, P.O. Box 28, 6700 AA Wageningen, The Netherlands

with $\mathbf{n}(\mathbf{x})$ the unit normal vector to $\mathcal{S}$, and the dynamic conditions,

$$\mathbf{t}_\alpha \cdot \boldsymbol{\tau}(\mathbf{v}) \cdot \mathbf{n} = 0, \qquad \mathbf{x} \in \mathcal{S}, \tag{2a}$$

$$p = 0, \qquad \mathbf{x} \in \mathcal{S}, \tag{2b}$$

are fulfilled. Here, $\mathbf{t}_\alpha(\mathbf{x})$ are orthogonal tangential unit vectors to $\mathcal{S}$ and $\boldsymbol{\tau}$ denotes the viscous stress tensor. In the derivation of the normal dynamic condition (2b) viscous effects have been ignored.

An equivalent formulation of the free-surface flow problem is obtained if the second dynamic condition (2b) is replaced by the quasi free-surface condition:

$$\mathbf{v} \cdot \boldsymbol{\nabla} p = 0, \qquad \mathbf{x} \in \mathcal{S}. \tag{2b*}$$

Condition (2b*) results from a combination of the kinematic and dynamic condition. In [1] it is shown for perturbations of a uniform flow in a channel of unit depth that the Navier-Stokes equations subject to boundary condition (2b*) allow gravity wave solutions that satisfy the usual dispersion relation. Denoting by $\mathcal{C}(\mathcal{V}, \mathbf{v}, p)$ the problem corresponding to the steady (RA)NS equations on $\mathcal{V}$, with appropriate boundary conditions on fixed boundaries, $\partial\mathcal{V} \setminus \mathcal{S}$, and conditions (2a) and (2b*) on the free boundary, $\mathcal{S}$, we propose the following algorithm for solving the free-surface flow problem:

`initialize` $\mathcal{S}$; `solve` $\mathbf{v}, p$ `from` $\mathcal{C}(\mathcal{V}, \mathbf{v}, p)$;
`while` $(\|p(\mathbf{x})\|_{\mathcal{S}} > \epsilon)$`{update` $\mathcal{S} := \{\mathbf{x} + \mathbf{j}\mathrm{Fr}^2 p(\mathbf{x}) \mid \mathbf{x} \in \mathcal{S}\}$; `solve` $\mathbf{v}, p$ `from` $\mathcal{C}(\mathcal{V}, \mathbf{v}, p)$;`}`

Here, $\mathbf{j}$ stands for the vertical unit vector. The method relies on use of boundary condition (2b*) in each subproblem. Contrary to the kinematic condition (1) and the dynamic condition (2b), condition (2b*) permits a nonzero normal velocity and a nonconstant pressure at the approximate free boundary. Condition (2b*) is smooth in the sense that it holds to close approximation in a neighborhood of the actual free surface. Consequently, the adjustment of the boundary induces only small disturbances in the solution. Then, the update improves the approximation to the free-surface location. One may note that this approach is analogous to methods for solving steady free-surface potential flow, e.g., [4]. Results of the method for a testcase from [2] are presented in section 4.

3 Wave solutions of the discrete equations

To solve the free-surface (RA)NS problem numerically, at the expense of a discretization error, the continuous differential equations and boundary conditions are replaced by a system of discrete equations. By consistency, these discrete equations permit surface gravity wave solutions that obey a dispersion relation that is similar to that of the continuous equations. Analysis of the difference between solutions of the discrete equations and of the continuous equations yields valuable information on the properties of the discretization scheme. Moreover, such an analysis can serve in the development of discretization schemes with special behavior, e.g., low numerical damping of surface gravity waves. Subsequently, we present the results of such an analysis.

We consider perturbations of magnitude ϵ, $\epsilon \ll 1$, of a uniform horizontal flow with velocity V_0 in a channel of unit depth. Through asymptotic expansion and Fourier analysis, one can show that the system of equations resulting from the discretization of the incompressible NS equations and the boundary condition (2b*) on a uniform mesh with meshsize h, allows a steady gravity wave solution that is proportional to $\exp(\theta_1 x_1 + \theta_2 x_2)$, $(\theta_1, \theta_2) \in \mathbb{C}^2$, provided that the dispersion relation

$$V_0^2 \; \partial_{\mathrm{c}h}^1(\theta_1) \; \partial_{\mathrm{s}h}^1(\theta_1) = -\mathrm{Fr}^{-2} \frac{E(-\theta_2) - E(\theta_2)}{\dfrac{E(-\theta_2)}{\partial_{\mathrm{p}h}^2(\theta_2)} - \dfrac{E(\theta_2)}{\partial_{\mathrm{p}h}^2(-\theta_2)}} \tag{3}$$

is obeyed. Here, $\partial_{\mathrm{c}h}^1(\theta_1)$ denotes the symbol of the discrete approximation to the x_1-derivative of the velocity in the convective term of the momentum equations, $\partial_{\mathrm{s}h}^1(\theta_1)$ stands for the symbol of the x_1-derivative of the pressure in the quasi free-surface condition, $\partial_{\mathrm{p}h}^2(\theta_2)$ represents the symbol of the x_2-derivative of the pressure in the momentum equations and $E(\theta_2)$ denotes the symbol of the impermeability condition, $v = 0$, at the bottom boundary. Solutions of (3) should be compared to solutions of the dispersion relation corresponding to the continuous problem, viz., $(\theta_1, \theta_2) = (\mathrm{i}k, k)$ with $V_0^2 = \mathrm{Fr}^{-2} k^{-1} \tanh(k)$. Indeed, it can be verified by Taylor expansion of the Fourier symbols that for a consistent discretization, (θ_1, θ_2) by (3) approach $(\mathrm{i}k, k)$ as h tends to 0.

For the discretization employed in the numerical experiments, figure 1(l) displays the relative difference between the wavelength of a stationary wave solution of the continuous equations, $\lambda = 2\pi/k$, and the wavelength of a stationary wave solution of the discrete equations, $\lambda^h = 2\pi/\Im(\theta_1)$, with θ_1 according to (3), versus the Froude number, for various values of the meshwidth h. Figure 1(r) shows the associated wave attenuation per wavelength, $\nu^h = \exp(\Re(\theta_1)\, \lambda^h)$.

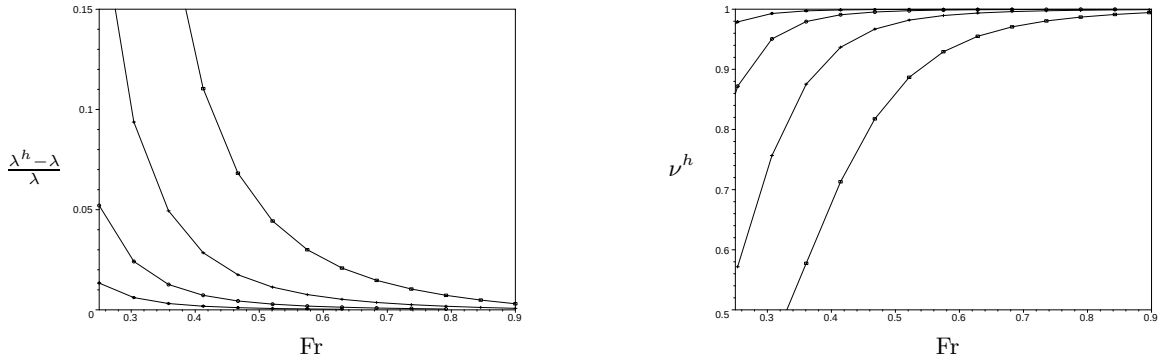

Figure 1: Relative difference in wavelength of stationary wave solutions of the discrete equations and of the continuous equations (l) and numerical wave damping (r), versus the Froude number for meshwidth $h = 1/10$ ($\Box$), $h = 1/20$ ($+$), $h = 1/40$ ($\circ$) and $h = 1/80$ ($\diamond$).

4 Numerical Experiments & Results

To test the algorithm described in section 2 and verify the results of the analysis presented in section 3, we conducted numerical experiments for the subcritical flow over a bump in a channel of unit depth at $\mathrm{Fr} = 0.43$ and $\mathrm{Re} = 3 \times 10^6$, with bumpheight $E = 0.2$, as described in [2] and, to reduce the non-linearity, with $E = 0.18$. The experiments were performed on grids with different meshwidths. In each case, exponential grid stretching was applied to resolve the boundary layer at the bottom. The steady RANS problems were solved by the method described in [3]. After each evaluation, the grid was adapted using relative vertical stretching and an initial estimate on the adapted grid was generated by linear interpolation from the solution on the previous grid.

Figure 2 displays the computed wave-elevation and the measurements from [2]. In [2] a (nondimensionalized) wavelength $\lambda = 1.1 \pm 10\%$ and an amplitude $\mathrm{a} = 4.5 \times 10^{-2} \pm 15\%$ is stated for the measurements of the trailing wave. The numerical results on a grid with horizontal meshwidth $h = 1/32$ yield $\lambda = 1.09$ and $\mathrm{a} = 6.4 \times 10^{-2}$. Hence, the computed amplitude is slightly overestimated and the wavelength is within the uncertainty interval.

The table in figure 3 lists the wavelength and the wave-attenuation according to the numerical results, for $E = 0.18$, and according to dispersion relation (3). The numerical results and the predictions by (3) exhibit good agreement. The differences are within the uncertainty that is introduced by determining the wavelength and the wave-attenuation from the computed wave-elevation.

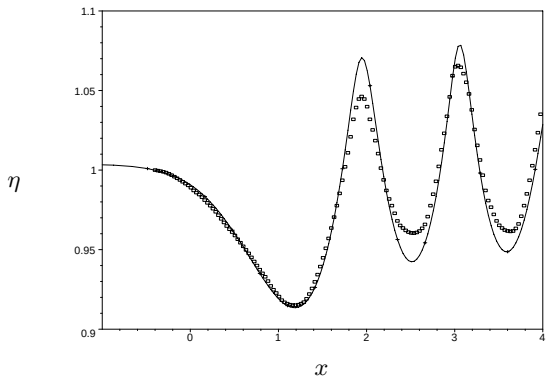

Figure 2: Computed wave elevation for $h = 1/32$ and measurements from [2].

	wavelength		attenuation	
h	comput.	analysis	comput.	analysis
1/10	1.30	1.27	0.74	0.75
1/20	1.22	1.19	0.94	0.95
1/40	1.18	1.17	0.99	0.99
1/80	1.17	1.16	1.00	1.00

Figure 3: Wavelength and wave attenuation of the numerical results, for $E = 0.18$, and by dispersion relation (3) for $h = 1/10, 1/20, 1/40, 1/80$.

Figure 4 displays the computed wave-elevation on the $h = 1/80$ grid after consecutive subproblem evaluations, when the initial estimate of the free boundary is the undisturbed surface. Observe that already after a single evaluation a wave-solution is obtained.

The table in figure 5 lists the pressure defect at the free surface after successive subproblem evaluations, with $\|p\|_{\mathcal{S}} = h \sum |p_i|$. The results reveal that 2 evaluations suffice to reduce the pressure defect by an order of magnitude. This indicates that the pressure defect and, hence, the boundary position converge linearly

with the number of subproblem evaluations. However, the evaluations become increasingly less expensive, because the error in the initial estimate that is obtained from the previous solution, decreases proportional with the pressure defect. As a consequence, for the testcase with $E = 0.18$, the computations were only marginally more expensive than a fixed domain computation; see also [5].

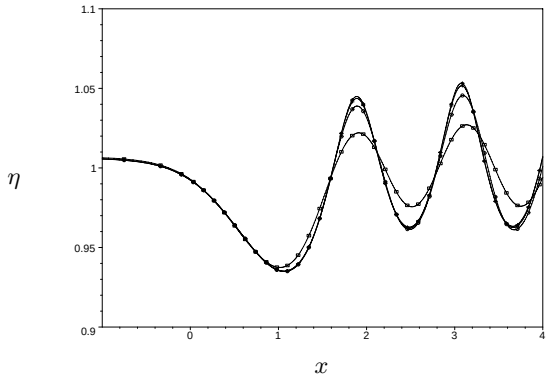

Figure 4: Wave elevation obtained after consecutive subproblem evaluations for $E = 0.18$ and $h = 1/80$.

#	$\|p\|_S$
1	5.38×10^{-1}
2	1.62×10^{-1}
3	3.46×10^{-2}
4	7.96×10^{-3}
5	2.47×10^{-3}
6	7.66×10^{-4}
7	2.17×10^{-4}
8	9.51×10^{-5}

Figure 5: Number of subproblem evaluations and corresponding pressure defect at the free surface for $E = 0.18$.

5 Conclusions

We presented a computational method for the efficient numerical solution of steady free-surface Navier-Stokes flow and a method for analyzing the properties of the discretization scheme.

The computational method solves a sequence of subproblems, with a quasi free-surface condition imposed at the free surface. After each subproblem evaluation, an improved approximation to the free-surface location is obtained. Numerical results were presented for the flow over a bottom-bump. The results agree well with measurements. Moreover, for the testcase presented, the method displays linear convergence of the boundary position with the number of subproblem evaluations. The results indicate that the method indeed permits efficient solution of steady free-surface Navier-Stokes flows.

The method for analyzing the properties of the discretization scheme employs asymptotic expansion techniques and Fourier analysis to determine the dispersion relation for the system of discrete equations. Results of the analysis were compared with numerical results on grids with different meshwidths. The comparison reveals good agreement between the predictions from the analysis and the numerical results. We expect that the method can serve in the development and assessment of discretization schemes.

References

[1] H. v. Brummelen, *Analysis of the incompressible navier-stokes equations with a quasi free-surface condition*, tech. rep., CWI, 1999. Available at `http://www.cwi.nl/static/publications/reports/MAS-1999.html`.

[2] J. Cahouet, *Etude numérique et experimentale du problème bidimensionnel de la résistance de vagues non-linéaire*, PhD thesis, ENSTA, Paris, 1984. (In French).

[3] M. Hoekstra, *Numerical Simulation of Ship Stern Flows with a Space-Marching Navier-Stokes Method*, PhD thesis, Delft University of Technology, Netherlands, 1999.

[4] H. Raven, *A Solution Method for the Nonlinear Ship Wave Resistance Problem*, PhD thesis, Delft University of Technology, Netherlands, 1996.

[5] H. Raven and H. v. Brummelen, *A new approach to computing steady free-surface viscous flow problems*, in 1st MARNET-CFD Workshop, Barcelona, 1999. Available at `http://www.marin.nl/projects/cph_parnassos_720.html`.